Journal of Nuclear Medicine, published on July 13, 2017 as doi:10.2967/jnumed.117.195107

Time Courses of Cortical Glucose Metabolism and Microglial Activity Across the Life-Span of Wild-Type Mice: A PET Study

by

Matthias Brendel[1*], Carola Focke[1*], Tanja Blume[1,2], Finn Peters[2], Maximilian Deussing[1], Federico Probst[1], Anna Jaworska[2,3], Felix Overhoff[1], Nathalie Albert[1], Simon Lindner[1], Barbara von Ungern-Sternberg[1], Peter Bartenstein[1], Christian Haass[4,5,6], Gernot Kleinberger[4,5], Jochen Herms[2,5,6], Axel Rominger[1,5]

[1]Dept. of Nuclear Medicine, University of Munich, Germany
[2]Center for Neuropathology and Prion Research, Ludwig-Maximilians-Universität München, Munich, Germany
[3]Laboratory of Neurodegeneration, International Institute of Molecular and Cell Biology, Warsaw, Poland
[4]Biomedical Center (BMC), Biochemistry, Ludwig-Maximilians-Universität München, Munich, Germany
[5]Munich Cluster for Systems Neurology (SyNergy), Munich, Germany
[6]DZNE - German Center for Neurodegenerative Diseases, Munich, Germany

* Contributed equally

Running Title: FDG- and TSPO-PET in aging WT mice
Word count: 4909

Correspondence:
Prof. Dr. Axel Rominger
Department of Nuclear Medicine
University of Munich, Germany
Phone: +49(0)89440074650
Fax: +49(0)89440077534
E-Mail: axel.rominger@med.uni-muenchen.de

Shared First authors:
Dr. Matthias Brendel (resident)
Department of Nuclear Medicine
University of Munich, Germany
Phone: +49(0)89440074646
Fax: +49(0)89440077646
E-Mail: Matthias.brendel@med.uni-muenchen.de

Carola Focke (student)
Department of Nuclear Medicine
University of Munich, Germany
Phone: +49(0)89440074646

Fax: +49(0)89440077646
E-Mail: carola.focke@med.uni-muenchen.de

ABSTRACT

Contrary to findings in human brain, ^{18}F-FDG PET shows cerebral hypermetabolism of aged wild-type (WT) mice relative to younger animals, supposedly due to microglial activation. Therefore, we used dual tracer µPET to examine directly the link between neuroinflammation and hypermetabolism in aged mice.

Methods:

WT mice (5-20 months) were investigated in a cross-sectional design using ^{18}F-FDG (N=43) and TSPO (^{18}F-GE180;N=58) µPET, with volume-of-interest and voxel-wise analyses. Biochemical analysis of plasma cytokine levels and immunohistochemical confirmation of microglial activity were also performed.

Results:

Age-dependent cortical hypermetabolism in WT mice relative to young animals aged five months peaked at 14.5 months (+16%,$p<0.001$), and declined to baseline at 20 months. Similarly, cortical TSPO binding increased to a maximum at 14.5 months (+15%,$p<0.001$), and remained high to 20 months, resulting in an overall correlation between 18F-FDG uptake and TSPO binding ($\beta=0.61$;$p<0.05$). Biochemical and immunohistochemical analyses confirmed the TSPO µPET findings.

Conclusion:

Age-dependent neuroinflammation is associated with the controversial observation of cerebral hypermetabolism in aging WT mice.

Key words:

TSPO PET; FDG PET; hypermetabolism; aging; wild-type mice;

INTODUCTION

Small animal positron emission tomography (μPET) in transgenic mouse models of Alzheimer's disease (AD) is a promising technique for monitoring disease-modifying treatments *in vivo* [1]. Clinical PET imaging with the glucose analogue 18F-fluoro-2-deoxy-*D*-glucose (18F-FDG) has become a standard procedure for detecting defects in cerebral glucose metabolism characteristic of AD and other brain diseases [2-4].

While confirmation of advanced AD to 18F-FDG-PET is unproblematic, preclinical stages of AD manifest in only subtle deviations from the cerebral metabolism typical of healthy brain. Furthermore, cerebral atrophy and relative hypometabolism both occur in healthy aging, notably in medial frontal regions [5-7] such that age dependent templates are needed for voxel-wise comparisons of 18F-FDG PET [8]. In contrast to the established findings of age-related hypometabolism in healthy human brain, previous preclinical studies found glucose hypermetabolism in aged wild-type (WT) mice relative to younger animals [9,10]. Microglial activation has been suggested as a possible driver for age-related 18F-FDG hypermetabolism in mice [11]. To test this hypothesis, we earlier undertook a dual tracer μPET study with 18F-FDG and also 18F-GE180, a tracer for the 18kDa translocator protein (TSPO), which is highly expressed at the outer mitochondrial membrane of activated microglia; preliminary results indicated an association between aged-dependent parallel increases TSPO binding and 18F-FDG uptake in transgenic AD model and also WT mice [12]. To characterize better this association, we have obtained 18F-GE180 and 18F-FDG μPET recordings in a large series of C57Bl/6 WT mice of various ages in a study of cross-sectional design. We predicted that there should be parallel age-dependent increases of both biomarkers, with regional co-localization of the increases in tracer uptake. Finally, we aimed to test if neuroinflammation and glucose

hypermetabolism correlate in individual mice, and also undertook additional biochemical analyses of inflammatory cytokines in brain and immunohistochemical analysis of microglial activation in order to cross-validate the μPET results.

MATERIAL AND METHODS

Animals and Study Design

All experiments were carried out in compliance with the National Guidelines for Animal Protection, Germany and with the approval of the regional animal care committee (Regierung Oberbayern), and were overseen by a veterinarian. Animals were housed in a temperature- and humidity-controlled environment with a 12-h light–dark cycle, with free access to food (Ssniff, Soest, Germany) and water. All studies were performed in female WT C57Bl/6 mice aged 5 to 20 months, purchased from Charles River (Sulzfeld, Germany).

μPET examinations were performed in a cross-sectional design for glucose metabolism (N=43) and TSPO (N=58). In particular, a subset of N=8 mice aged 8 and 14.5 months received both tracer examinations within a span of one week, so as to test directly for correlation of the two markers in individual mice. Another subset of mice (N=7 for glucose metabolism and N=8 for TSPO) underwent between two and four μPET investigations with each tracer (true longitudinal setting). All other mice were examined once with either FDG or TSPO PET.

Subsets of mice in the youngest and oldest groups were killed after scanning, followed by rapid brain removal and performance of ELISA for inflammatory cytokine levels in brain extracts, and also immunohistochemistry analyses. Group sizes by age and type of measurement are presented in **Table 1**.

Radiochemistry

Radiosynthesis of 18F-GE180 was performed as previously described [13], with slight modifications [12]. This procedure yielded a radiochemical purity exceeding 98%, and a specific activity of 1400±500 GBq/µmol at end of synthesis. 18F-FDG was purchased commercially.

µPET Data Acquisition and Reconstruction

All mice were anesthetized with isoflurane (1.5%, delivered at 3.5 l/min) and placed in the aperture of the Siemens Inveon DPET, as described previously [14]. Further details are provided in the **Supplement**.

µPET Data Analyses

All single-frame static datasets (30-60 min or 60-90 min) were co-registered to an MRI mouse atlas [15] by a manual rigid-body transformation using the PMOD fusion tool (V3.5, PMOD Technologies Ltd.) after anonymizing the mouse identity to the reader. Accurate initial alignment was verified by a second experienced reader. In the second step, a reader-independent, fine co-registration to tracer-specific templates was performed [16]. These templates had been generated by averaging all available age-specific PET scans of a single tracer after minor spatial re-registrations to assure optimal overlapping. Here, the initial manual µPET-to-MRI atlas fusion images were spatially normalized to the tracer-specific templates by a non-linear brain normalization tool in PMOD (equal modality; smoothing by 0.6 mm; nonlinear warping; 16 iterations; frequency cut-off 3; regularization 1.0; no thresholding). The concatenation of both

transformations was then applied to µPET images in the native space, so as to obtain optimal resampling with a minimum of interpolation.

A bilateral frontal cortical target volume-of-interest (VOI; comprising 24 mm³ in total), was used for both tracers. The bilateral striatum VOI (21 mm³) were applied as a representative forebrain region with low TSPO density. Bilateral hippocampal (comprising 10 mm³ in total) and parietal (comprising 14 mm³ in total) VOIs were used for extended analyses. The previously-validated oval shaped reference tissue VOI containing white matter of the cerebellum and the brainstem (comprising 29 mm³; [12]) was used for SUV normalization of 18F-GE180 µPET images. Based on our previous experience, the entire cerebellum (comprising 65 mm³) was used for scaling of 18F-FDG data. Target-to-reference tissue standardized-uptake-values ratios (SUVR) were calculated for 18F-GE180 ($SUVR_{Target/WM}$) and 18F-FDG ($SUVR_{Target/CBL}$).

SPM analysis and dice coefficient

For both tracers, whole-brain voxel-wise comparisons between young (5-6 months) and moderately aged (14.5 months) WT mice were performed by statistical parametric mapping (SPM) using SPM5 routines (Wellcome Department of Cognitive Neurology, University College London, UK) implemented in MATLAB (version 7.1), as adapted from Sawiak et al. [17] for mouse data. These two age groups were selected after completing the VOI-based analysis as they represented the maximum age-dependent increase for both tracers. T-Score maps of the age group contrasts were all corrected for multiple comparisons (FDR-corrected) at a significance level of $p < 0.05$. Significant areas were binarized by the respective T-score threshold for each tracer and used to define the overlap of regions with specific increases in tracer uptake with age.

The Sørensen–Dice index for comparing the similarity of two samples [18] was calculated for the T-statistic maps of longitudinal 18F-GE180 and 18F-FDG uptake differences (14.5 months > 5-6 months) to assess the spatial agreement of the pseudo-longitudinal binding increases with age.

Immunohistochemistry: Acquisition and Image Analysis

Details are provided in the Supplement.

Biochemical Analyses of Cytokines

Details are provided in the Supplement.

Statistics

Statistical analyses of PET data were performed in SPSS (SPSS Version 23, SPSS Software, IBM, New York). Group comparisons of VOI-based µPET results between different age groups were assessed by ANOVA with Tukey post hoc correction. For correlation analyses, Pearson's coefficients of correlation (R) were calculated. Multiple regression analysis was performed to investigate the association of cortical glucose metabolism and microglial activation with age as a fixed effect. The standardized regression coefficients (β) are reported. Statistics of histological and volumetric analyses were calculated in Prism v5.04 (GraphPad Software, San Diego, CA, USA). Analysis of the difference in the volumes of cortex and motor cortex between aged and young mice was performed using an unpaired Student t-test. Other intergroup comparisons were performed using the two-tailed Student t-test. The Kolmogorov-Smirnov test (KS-test) was used to confirm the statistical results based on Student t-test.

The KS-test enables determining if two datasets differ significantly, based on statistics that measure the greatest distance between the empirical distribution function (EDF) of the univariate dataset and the comparison step function of the second dataset. Here, we compared the fraction of different soma volumes of microglia between young and aged mice.

For all comparisons, a threshold of $p<0.05$ was considered to be significant for rejection of the null hypothesis.

RESULTS

Dual Tracer µPET analyses

For both tracers a significant cortical increase was already observed between 5-6 and 8 month old C57Bl/6 mice (18F-FDG: +10%, $p<0.005$; 18F-GE180: +8%, $p<0.005$, **Fig. 1AB**). 14.5 month old C57Bl/6 mice indicated parallel cortical increases for glucose metabolism and TSPO binding compared to 5-6 month old animals (18F-FDG: +16%, $p<0.001$; 18F-GE180: +15%, $p<0.001$). In the most aged mice (≥ 14.5 months) there was a slowly descending plateau for the TSPO SUVR, whereas 18F-FDG uptake declined from a peak to that seen in the youngest group (20 vs. 14.5 months: -12%, $p<0.001$). Findings of longitudinal imaging were congruent with cross-sectional data (**Supplemental Fig. 2**).

Striatal TSPO binding increased non-significantly from 5-6 to 8 months of age (+5%), and the only significant difference was observed in the contrast between 5-6 and 20 months (+7%, $p<0.05$, **Fig. 1C**). Glucose metabolism in the striatum increased with age, peaking at 14.5 months (14.5 vs. 5-6 months: +9%, $p<0.01$), and then dropping below the baseline level at the age of 20 months (20 vs 5-6 months: -7%, p=n.s.; 20 vs

16 months: -14%, p<0.01; **Fig. 1D**). Hippocampal and parietal findings of TSPO binding and glucose metabolism are provided **Supplemental Figure 3**.

Correlation Analyses of PET studies

In a subset of C57Bl/6 mice (8 and 14.5 months; N=8 each) both µPET measurements were conducted within the same week. In these mice, the cortical SUVR results for 18F-FDG and 18F-GE180 correlated within individual mice (R=0.69, p<0.005, **Fig. 2**). We next inquired whether cortical glucose metabolism is associated with TSPO binding independently of age. To this end, we performed a multiple regression analysis with 18F-FDG SUVR as an outcome variable, with 18F-GE180 SUVR as predictor, and with introduction of age as a covariate. In this analysis, cortical 18F-FDG SUVR was significantly associated with cortical 18F-GE180 SUVR (β=0.61; p<0.05), after adjusting for age. Striatal uptake of the two tracers did not correlate with each other (R=0.06, p=n.s.).

Voxel-wise Analyses of PET Studies

SPM indicated a clear spatial relationship between age-dependent alterations of neuroinflammation and glucose metabolism as measured *in vivo* by µPET. C57Bl/6 mice revealed a cortically pronounced increase of TSPO binding (**Fig. 3A**) and glucose metabolism (**Fig. 3B**) between 5-6 and 14.5 months. In particular, the longitudinal increases of both tracers exceeding the threshold for FDR-correction (p<0.01) overlapped in 36 mm³ of the entire neocortical brain volume (primary and secondary motor areas, primary somatosensory areas, anterior cingulate cortex, **Fig. 3C**). Glucose metabolism comprised additional longitudinal increases in a further 37 mm³ of the brain

volume, encompassing g mostly lateral cortical areas and minor clusters in subcortical areas (thalamus, striatum). A larger volume showed a specific increase of 18F-GE180 signal without elevated 18F-FDG uptake (68 mm^3; predominantly subcortical areas: midbrain, thalamus, striatum). The calculated Sørensen-Dice coefficient confirmed a high similarity of 54.5% between the parametric age-dependent increase maps of 18F-GE180 and 18F-FDG.

Immunohistochemistry and 3D Volumetric Analyses

We confirmed the immunohistochemical correlates of increasing TSPO binding evident to 18F-GE180 µPET in older WT mice. The volume-% of Iba1-positive microglial soma was significantly elevated in aged WT mice when compared to the young cohort (0.44±0.03% vs. 0.33±0.02%; $p<0.05$.; **Fig. 4A**), whereas volume-% of Iba1-positive fibers did not reveal a significant difference (2.66±0.05% vs. 2.68±0.08%; p=n.s.; **Fig. 4B**). Density of Iba1-positive microglia cells was equal between aged and young WT mice ($2.2E^{-5}/µm^3$ vs. $2.2E^{-5}/µm^3$; p=n.s.; **Fig. 4C**). By plotting all analyzed soma volumes against their frequency, we identified a clear shift towards larger volumes for aged WT mice (**Fig. 4D**). Indeed, larger soma volumes in aged WT mice were discernible to visual inspection of the micrographs (compare young and aged in **Fig. 4E**). 3D volumetric analyses revealed identical cortical volumes for young and aged mice (29.0±1.8 versus 28.3±1.6 mm^3, p=n.s.; **Supplemental Fig. 4**).

ELISA

Biochemical analysis of WT brains confirmed an age-dependent neuroinflammation as indicated by elevated cytokines at 19-20 months compared to 6

months: IL-1 (+63%; $p<0.05$ **Fig. 5A**), IL-6 (+23%; $p<0.005$ **Fig. 5B**) and KC/GRO (+91%; $p<0.05$ **Fig. 5C**).

DISSCUSION

This is the first large scale *in vivo* study aiming to uncover molecular and cellular relationships between glucose metabolism and microglial activation during aging of WT mice. We performed dual *in vivo* µPET with the novel TSPO tracer 18F-GE180 and the commonly used glucose metabolism tracer 18F-FDG in WT mice in conjunction with biochemical assessments of neuroinflammatory markers. This analysis revealed close temporal and spatial correlations between the age-dependent increases of both µPET biomarkers. Immunohistochemical and biochemical assessments confirmed the TSPO µPET findings, thus providing consistent evidence that the previously described cortical hypermetabolism in aged WT mice is accompanied by increasing neuroinflammation. These preclinical findings substantiate a contribution of microglial activation in aging WT mice to the net energy balance of brain.

As in previous µPET studies [9,10,19] we found an increase of 18F-FDG uptake in the cortex of WT mice between 5-6 and 14.5 months of age. To date the reason for this discrepancy with the age-related decrease of 18F-FDG metabolism in human cerebral cortex [5-7], has been a matter of speculation. Our *in vivo* findings in WT C57Bl/6 mice show a clear temporal and spatial association between neuroinflammation to TSPO µPET and cortical glucose metabolism, likewise assessed by µPET. The present finding of age-related increased cortical TSPO signal is strongly supported by a recent study [20], who also reported an age-dependent increase of 18F-GE180 uptake in WT mice from 4 to 26 months *in vivo*, as confirmed by *ex vivo* autoradiography. Our *in vivo* finding of

increased neuroinflammation in aged WT mice was confirmed by *post mortem* assessments of elevated immunostaining of microglia cells and proinflammatory cytokine levels in brain of aged mice. Interestingly, the microglial cell and Iba1-positive fiber densities were unchanged, but the diameter of microglia soma was higher in the aged mice (**Fig. 4**). These findings are in line with an earlier report on microglia in C57Bl/6J-Iba1-eGFP mice, in which the authors found increasing soma diameter and decreasing microglial filament length in older mice [21]. We note that the age of our oldest mice (19-20 months) fell midway between the adult (11-12 months) and aged (26-27 months) groups of their study. Importantly, increased soma volume is an index of higher activation states of microglia [22]. While our TSPO immuinohistochemical staining did not afford quantitation of off-target binding in vessels, it clearly indicated a co-localization of TSPO positivity in microglial soma and only sparse staining in fibers (**Supplemental Fig. 5**).

This dissociation between soma and ramifications is unsurprising, as TSPO is localized at the outer membrane of mitochondria [23], which are mainly confined to the cell bodies, sparsely present in thick dendrites, and nearly absent from distal dendrites. Although we did not directly test this link with organelles, it seems plausible that enlarged soma of activated microglial aged mice should contain more mitochondria, which together probably contribute to elevated TSPO activity and glucose consumption. Microglia, as the resident macrophages of brain are a highly mobile cell population [24], and are highly dependent upon glucose, and to a lesser extent on fatty acids for energy metabolism [25]. At present, the contribution of microglia to the cortical energy budget is unknown; this might be ascertainable by high resolution electron microscopy in conjunction with ^{3}H2-deoxyglucose autoradiography, as in early studies of cellular

metabolism in invertebrate ganglia [26]. However, it seems certain that microglial activation as occurs in aging WT mice may become a significant component of the brain total energy budget.

It remains uncertain why the trajectories of cortical glucose metabolism with age differ in rodent and human brain. Human *post mortem* data have revealed larger soma volumes and more proinflammatory transcripts in senescent microglia [27], thus matching the phenotype in the present study. Interestingly, microglial activation in the aged human brain makes the hippocampus more vulnerable to cognitive decline [28]. Additionally, senescent microglia are primed to be more reactive to inflammatory stimuli, thus tending to overproduce pro-inflammatory cytokines for an extended period, which results in maladaptive sickness responses [29]. Importantly, not only general markers of neuroinflammation, but specifically TSPO binding has been shown to increase during healthy human aging [30]. In accord with that observation, we see increasing TSPO signal during normal aging in WT mice, which seemingly reaches a plateau at 20 months of age. Interestingly, the largest step in increase of TSPO (and FDG) signal was observed between young mice at 5-6 months and 8 months of age, which is rather precipitous in this brief interval. We can only speculate about the reason for this transition, which may be related to environmental stresses arising from transfer from the breeding laboratory to our facility [31].

The well-known cortical hypometabolism of healthy aged humans [7] was distinctly absent in aging WT mice. This disagreement might arise from the different life expectancy of mice and humans; the declining cerebral energy metabolism is first evident in human brain by the age of 50 years [7], which is mirrored by declines in oxygen extraction fraction [32]. Middle age for humans might be compared to an age of 16 months

in mice [33]. Indeed, present data indicated a plateau after 14.5 months of age for cortical 18F-GE180 binding, whereas the peak in 18F-FDG uptake is followed at 20 months by a significant decrease to levels typical of young mice (**Fig. 1**). Insofar as 18F-FDG uptake is most likely the composite of “normal” neuronal and astroglial glucose metabolism [34] plus inflammatory related microglial activation, we interpret the age-dependency to reflect the sum of the three cellular components, each with their own trajectory. The evident uncoupling of glucose metabolism and microglial activity in mice aged >14.5 months is potentially related to the onset of age-dependent neurodegeneration, such that neuronal metabolism becomes the driver for net changes in glucose consumption in aged mice. Indeed, striatal glucose metabolism at 20 months had decreased to even below the 5-6 month baseline data, which supports the above interpretation, as the microglial proportion of the 18F-FDG signal is likely lower for this region (compare regional TSPO activity in **Fig. 1C** and **Fig. 1A**). Thus, the striatal glucose metabolism probably decreases due to age dependent neurodegeneration, which is not masked by increasing microglial glucose consumption. It needs to be elucidated in future studies if there is a causal relationship between early cortical microglial activation and later decreases in glucose metabolism of the entire forebrain. Our findings predict a further decrease of cortical glucose metabolism in very aged mice (>20 months). However, due to increasing drop-out rates, we decided to confine our investigation to a younger age range, which is typical for most of the earlier µPET studies.

At least in human neurodegenerative disease there is an inverse relationship between cortical TSPO binding and 18F-FDG uptake [35]. However, PET studies do not distinguish the cellular site of TSPO binding or metabolism; another investigation suggests that glucose consumption of inflammatory cells could mask the true extent of

specifically neuronal metabolism deficits in the aging brain [11]. In regional analysis of our WT mice we confirmed a high spatial similarity by the calculated Sørensen-Dice coefficient (54.5%), which fits to the proposed colocalization of the increases in the two markers. This conclusion has implications for our previous findings in a transgenic PS2APP AD mouse model with known cognitive decline despite elevated cortical glucose metabolism [12]. In light of the current findings, the elevated glucose metabolism in that study was likely driven by the pronounced microglial response), which would have masked a decrease of neuronal glucose consumption. As noted above, electron microscopy in conjunction with ^{3}H2-deoxyglucose autoradiography could resolve the microglial contribution to brain energy budget.

Limitations

Global changes in 18F-FDG uptake during healthy aging of mice are possibly missed as they would be masked by the reference region scaling of the applied SUVR method; absolute quantitation of the cerebral metabolic rate for glucose (CMR_{glc}) relative to an image-derived input function [36] might give a clearer depiction of age-related changes. Regional cerebral blood flow is known to influence (semi-quantitative) assessments of glucose metabolism using the current SUVR method [37], such that age-dependent perfusion changes may be a confounder in our 18F-FDG analyses. Nonetheless, SUVR methods are standard practice in clinical 18F-FDG PET imaging [38], which may justify the design of the present preclinical study. A true longitudinal setting might be preferable to the present cross-sectional design, but would have entailed as many as 10 µPET examinations for each biomarker in each mouse; this would be logistically difficult due to the incidence of dropouts

CONCLUSION

We demonstrated an age-dependent and highly colocalized increase of cortical glucose metabolism to 18F-FDG and TSPO binding to 18F-GE180 µPET in WT mice aged from 5 to 14.5 months. Age-dependent cortical neuroinflammation potentially explains the widely described but controversially discussed hypermetabolism in aged C57/BL6 mice. The contribution of activated microglia to the brain energy budget should be considered in 18F-FDG PET studies of AD and other neuroinflammatory conditions. Furthermore, present findings emphasize the need for age-matched controls in preclinical research of TSPO activity and glucose metabolism.

DISCLOSURE

The study was financially supported by the SyNergy Cluster (J.H.,P.B.,C.H., and A.R.).

ACKNOWLEDGEMENTS

Manuscript editing was provided by Inglewood Biomedical Editing. GE180 cassettes were purchased from GE.

REFERENCES

1. Brendel M, Jaworska A, Herms J, et al. Amyloid-PET predicts inhibition of de novo plaque formation upon chronic gamma-secretase modulator treatment. *Mol Psychiatry.* 2015;20:1179-1187.

2. Bohnen NI, Djang DS, Herholz K, Anzai Y, Minoshima S. Effectiveness and safety of 18F-FDG PET in the evaluation of dementia: a review of the recent literature. *J Nucl Med.* 2012;53:59-71.

3. Minoshima S, Frey KA, Koeppe RA, Foster NL, Kuhl DE. A diagnostic approach in Alzheimer's disease using three-dimensional stereotactic surface projections of fluorine-18-FDG PET. *J Nucl Med.* 1995;36:1238-1248.

4. Tripathi M, Tripathi M, Damle N, et al. Differential diagnosis of neurodegenerative dementias using metabolic phenotypes on F-18 FDG PET/CT. *Neuroradiol J.* 2014;27:13-21.

5. Hsieh TC, Lin WY, Ding HJ, et al. Sex- and age-related differences in brain FDG metabolism of healthy adults: an SPM analysis. *J Neuroimaging.* 2012;22:21-27.

6. Yoshizawa H, Gazes Y, Stern Y, Miyata Y, Uchiyama S. Characterizing the normative profile of 18F-FDG PET brain imaging: sex difference, aging effect, and cognitive reserve. *Psychiatry Res.* 2014;221:78-85.

7. Kakimoto A, Ito S, Okada H, Nishizawa S, Minoshima S, Ouchi Y. Age-Related Sex-Specific Changes in Brain Metabolism and Morphology. *J Nucl Med.* 2016;57:221-225.

8. Ishii K, Willoch F, Minoshima S, et al. Statistical brain mapping of 18F-FDG PET in Alzheimer's disease: validation of anatomic standardization for atrophied brains. *J Nucl Med.* 2001;42:548-557.

9. de Cristobal J, Garcia-Garcia L, Delgado M, Perez M, Pozo MA, Medina M. Longitudinal assessment of a transgenic animal model of tauopathy by FDG-PET imaging. *J Alzheimers Dis.* 2014;40 Suppl 1:S79-89.

10. Poisnel G, Herard AS, El Tannir El Tayara N, et al. Increased regional cerebral glucose uptake in an APP/PS1 model of Alzheimer's disease. *Neurobiology of aging.* 2012;33:1995-2005.

11. Backes H, Walberer M, Ladwig A, et al. Glucose consumption of inflammatory cells masks metabolic deficits in the brain. *Neuroimage.* 2016;128:54-62.

12. Brendel M, Probst F, Jaworska A, et al. Glial Activation and Glucose Metabolism in a Transgenic Amyloid Mouse Model: A Triple Tracer PET Study. *J Nucl Med.* 2016.

13. Wickstrom T, Clarke A, Gausemel I, et al. The development of an automated and GMP compliant FASTlab Synthesis of [(18) F]GE-180; a radiotracer for imaging translocator protein (TSPO). *Journal of labelled compounds & radiopharmaceuticals.* 2014;57:42-48.

14. Rominger A, Mille E, Zhang S, et al. Validation of the octamouse for simultaneous 18F-fallypride small-animal PET recordings from 8 mice. *J Nucl Med.* 2010;51:1576-1583.

15. Dorr A, Sled JG, Kabani N. Three-dimensional cerebral vasculature of the CBA mouse brain: a magnetic resonance imaging and micro computed tomography study. *Neuroimage.* 2007;35:1409-1423.

16. Overhoff F, Brendel M, Jaworska A, et al. Automated Spatial Brain Normalization and Hindbrain White Matter Reference Tissue Give Improved [(18)F]-Florbetaben PET Quantitation in Alzheimer's Model Mice. *Frontiers in neuroscience.* 2016;10:45.

17. Sawiak SJ, Wood NI, Williams GB, Morton AJ, Carpenter TA. Voxel-based morphometry in the R6/2 transgenic mouse reveals differences between genotypes not seen with manual 2D morphometry. *Neurobiology of disease.* 2009;33:20-27.

18. Forster S, Grimmer T, Miederer I, et al. Regional expansion of hypometabolism in Alzheimer's disease follows amyloid deposition with temporal delay. *Biological psychiatry.* 2012;71:792-797.

19. Brendel M, Probst F, Jaworska A, et al. Glial Activation and Glucose Metabolism in a Transgenic Amyloid Mouse Model: A Triple-Tracer PET Study. *J Nucl Med.* 2016;57:954-960.

20. Liu B, Le KX, Park MA, et al. In Vivo Detection of Age- and Disease-Related Increases in Neuroinflammation by 18F-GE180 TSPO MicroPET Imaging in Wild-Type and Alzheimer's Transgenic Mice. *J Neurosci.* 2015;35:15716-15730.

21. Hefendehl JK, Neher JJ, Suhs RB, Kohsaka S, Skodras A, Jucker M. Homeostatic and injury-induced microglia behavior in the aging brain. *Aging Cell.* 2014;13:60-69.

22. Cunningham CL, Martinez-Cerdeno V, Noctor SC. Microglia regulate the number of neural precursor cells in the developing cerebral cortex. *J Neurosci.* 2013;33:4216-4233.

23. Papadopoulos V, Baraldi M, Guilarte TR, et al. Translocator protein (18kDa): new nomenclature for the peripheral-type benzodiazepine receptor based on its structure and molecular function. *Trends Pharmacol Sci.* 2006;27:402-409.

24. Nimmerjahn A, Kirchhoff F, Helmchen F. Resting microglial cells are highly dynamic surveillants of brain parenchyma in vivo. *Science.* 2005;308:1314-1318.

25. Kalsbeek MJ, Mulder L, Yi CX. Microglia energy metabolism in metabolic disorder. *Mol Cell Endocrinol.* 2016;438:27-35.

26. Kai Kai MA, Pentreath VW. High resolution analysis of [3H]2-deoxyglucose incorporation into neurons and glial cells in invertebrate ganglia: histological processing of nervous tissue for selective marking of glycogen. *J Neurocytol.* 1981;10:693-708.

27. Wolf SA, Boddeke HW, Kettenmann H. Microglia in Physiology and Disease. *Annu Rev Physiol.* 2016.

28. Ojo JO, Rezaie P, Gabbott PL, Stewart MG. Impact of age-related neuroglial cell responses on hippocampal deterioration. *Front Aging Neurosci.* 2015;7:57.

29. Matt SM, Johnson RW. Neuro-immune dysfunction during brain aging: new insights in microglial cell regulation. *Curr Opin Pharmacol.* 2016;26:96-101.

30. Gulyas B, Vas A, Toth M, et al. Age and disease related changes in the translocator protein (TSPO) system in the human brain: positron emission tomography measurements with [11C]vinpocetine. *Neuroimage.* 2011;56:1111-1121.

31. Walker FR, Nilsson M, Jones K. Acute and chronic stress-induced disturbances of microglial plasticity, phenotype and function. *Curr Drug Targets.* 2013;14:1262-1276.

32. Aanerud J, Borghammer P, Chakravarty MM, et al. Brain energy metabolism and blood flow differences in healthy aging. *Journal of cerebral blood flow and metabolism : official journal of the International Society of Cerebral Blood Flow and Metabolism.* 2012;32:1177-1187.

33. Flurkey K, Currer J, Harrison D. *The Mouse in Aging Research*. Burlington, MA: American College Laboratory Animal Medicine (Elsevier); 2007.

34. Zimmer ER, Parent MJ, Souza DG, et al. [18F]FDG PET signal is driven by astroglial glutamate transport. *Nature neuroscience.* 2017;20:393-395.

35. Edison P, Ahmed I, Fan Z, et al. Microglia, amyloid, and glucose metabolism in Parkinson's disease with and without dementia. *Neuropsychopharmacology.* 2013;38:938-949.

36. Xiong G, Paul C, Todica A, Hacker M, Bartenstein P, Boning G. Noninvasive image derived heart input function for CMRglc measurements in small animal slow infusion FDG PET studies. *Phys Med Biol.* 2012;57:8041-8059.

37. Backes H, Walberer M, Endepols H, et al. Whiskers area as extracerebral reference tissue for quantification of rat brain metabolism using (18)F-FDG PET: application to focal cerebral ischemia. *J Nucl Med.* 2011;52:1252-1260.

38. Dukart J, Mueller K, Horstmann A, et al. Differential effects of global and cerebellar normalization on detection and differentiation of dementia in FDG-PET studies. *Neuroimage.* 2010;49:1490-1495.

Figures

Figure 1:

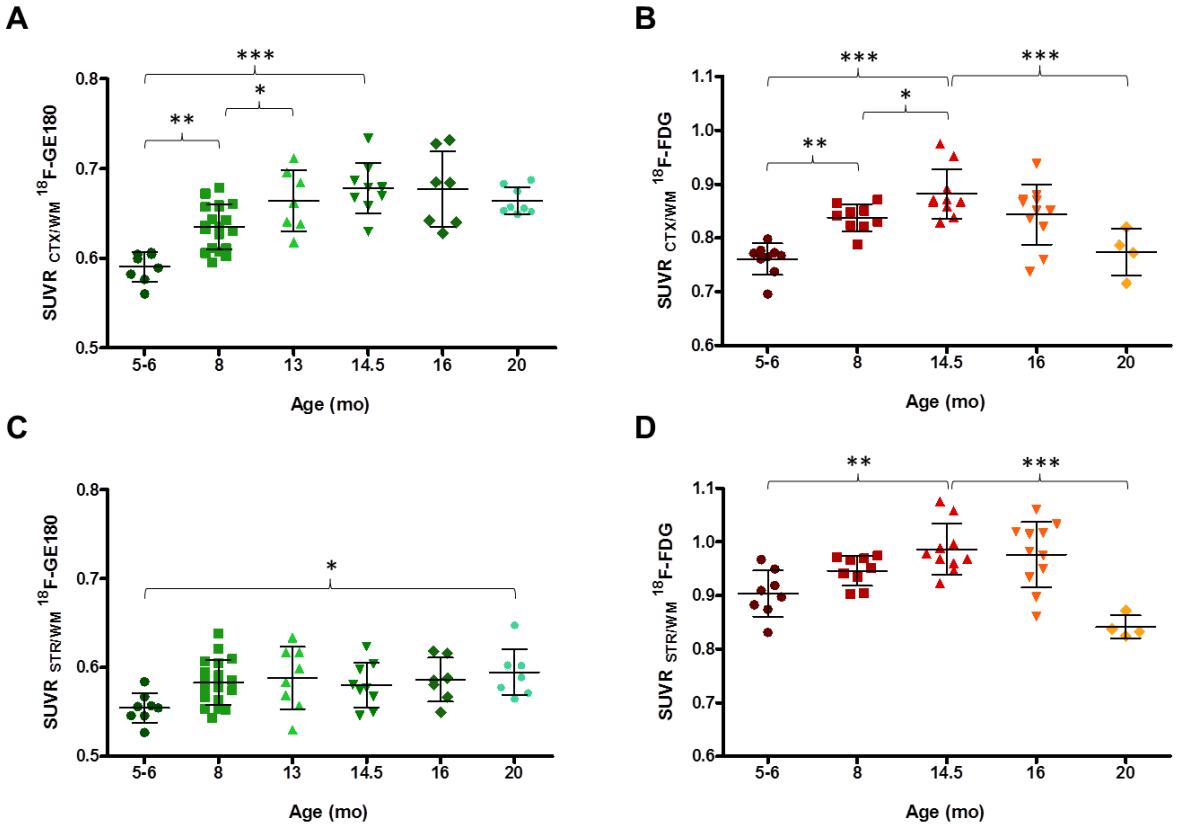

Plots show mean (±SD) cortical SUVR of (**A**) 18F-GE180 and (**B**) 18F-FDG in C57Bl/6 mice at different ages. Corresponding striatal SUVR values are provided in (**C**) and (**D**). Significant differences between subgroups are marked by *p<0.05, **p<0.01, ***p<0.001; ANOVA with Tukey post hoc correction.

Figure 2:

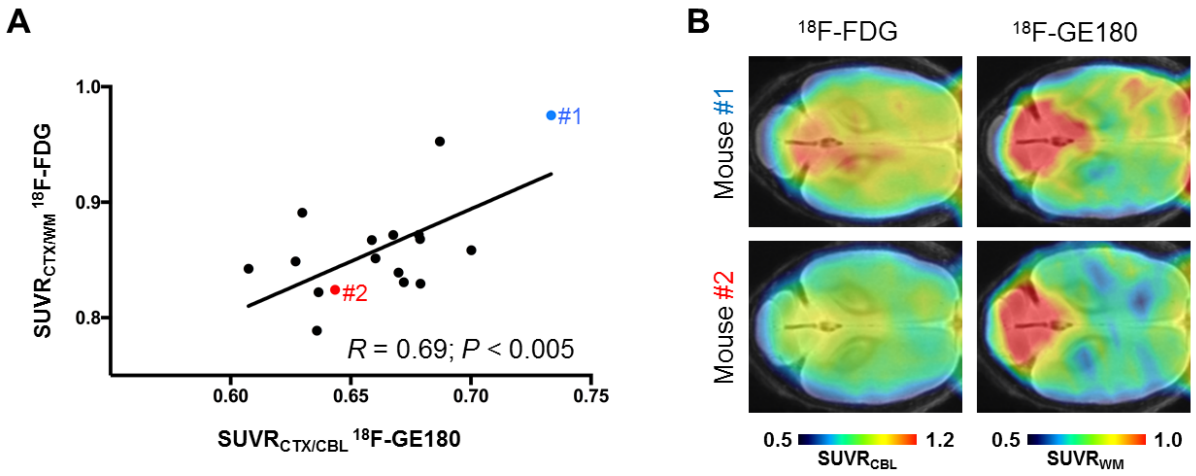

Correlation analysis between cortical TSPO binding and glucose metabolism in a subset of C57Bl/6 mice (N=16) in which both PET measurements were conducted within the same week. Images from two representative mice aged 14.5 months are illustrated as horizontal slices through the neocortex co-registered with a T1 MRI template (red and green circles in the plot). Mouse #1 indicated high cortical glucose metabolism and high TSPO binding, whereas mouse #2 had comparably low cortical glucose metabolism and low TSPO binding.

Figure 3:

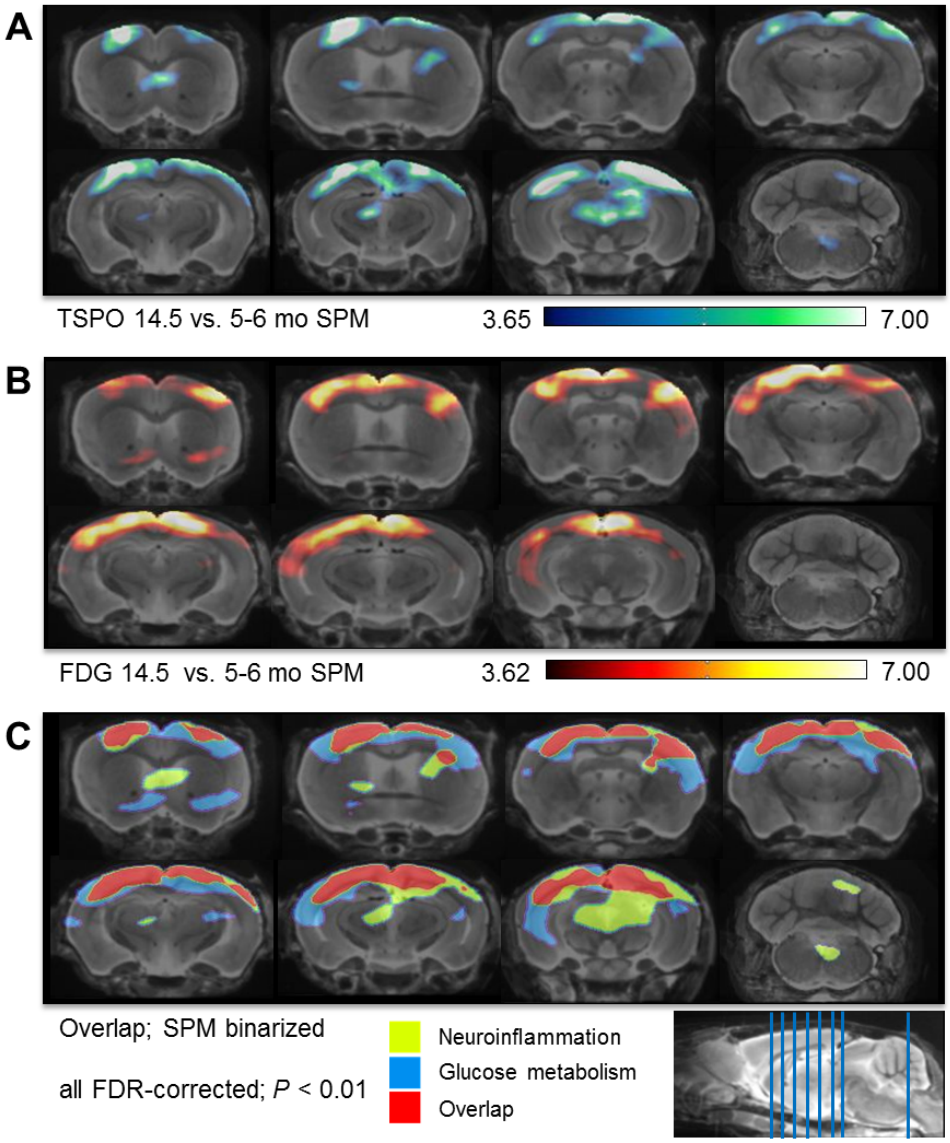

Voxel-wise regional increases of radiotracer uptake in aged compared to young C57Bl/6 mice for TSPO binding (**A**) and glucose metabolism (**B**) as assessed by SPM. (**C**) Binarized specific increases in 18F-GE180 uptake, indicating microglial activation (green), binarized specific increases in 18F-FDG uptake, indicating hypermetabolism (blue), and areas of overlapping increases for both tracers (red) are projected upon coronal slices of an MRI mouse atlas, as depicted in planes on the mid-sagittal slice. All p<0.01, FDR-corrected.

Figure 4:

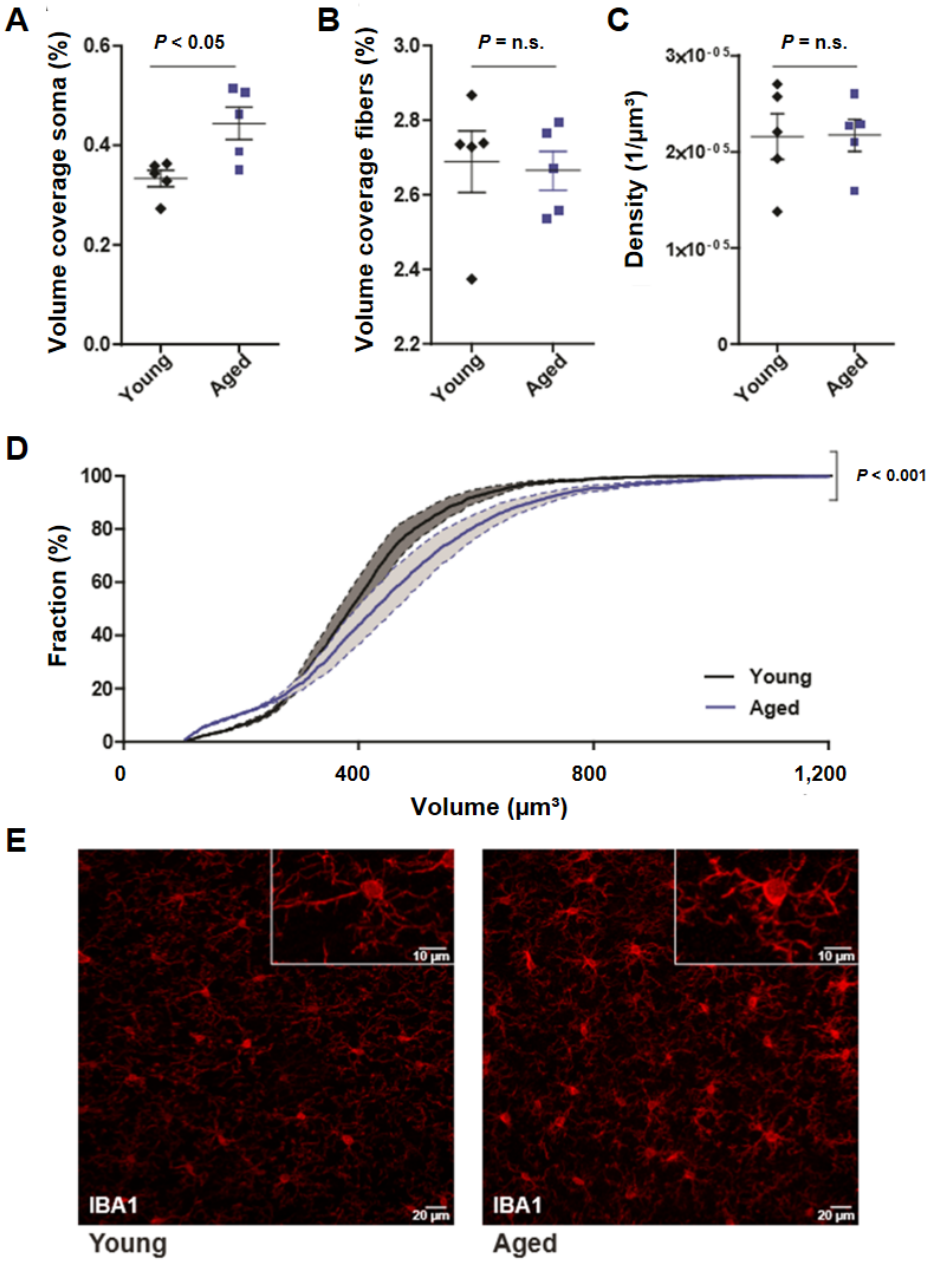

Quantification of volume coverage of soma (**A**) and fibers (**B**) of Iba1-positive microglia showed an increase in soma volume in aged (19-20 months old) WT mice, whereas no change in fiber volumes could be observed. (**C**) Quantification of microglia density showed no difference between young and aged mice. (**D**) Cumulative sum of soma volumes indicate a shift towards larger volumes in aged mice. (**E**) Confocal images of Iba1 immunostainings in young and aged mouse cortex. Data present as mean ±SEM, n=5 per group, two-tailed student t-test.

Figure 5:

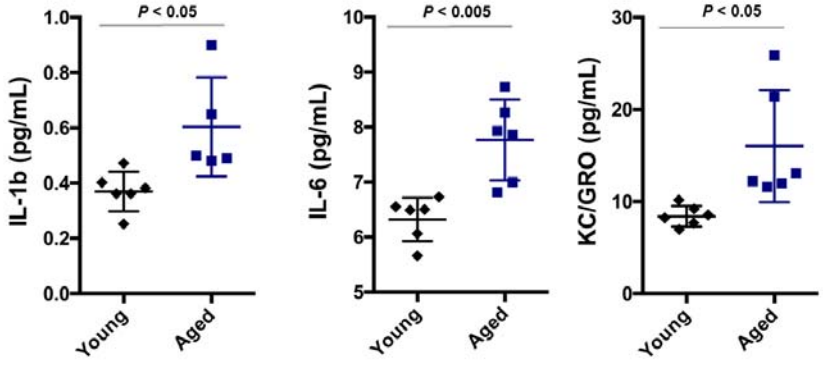

Summary of cytokine findings in WT mice aged 6 and 19-20 months**.** Bar graphs show mean ±SD for IL-1b levels and IL-6 levels as well as KC/GRO levels.

Table 1: Study overview

Age (mo)	PET 18F-GE180 (N)	PET 18F-FDG (N)	ELISA IL1b, IL6, KC/GRO (N)	Immunohistochemistry Iba1 (N)
5-6	8	9	6	5
8	19	9		
13	7			
14.5	9	10		
16	7	11		
19-20	8	4	6	5

Dual µPET experiments, ELISA and immunohistochemistry were performed in groups of WT C57Bl/6 mice at various ages.